European Cells and Materials Vol. 26 2013 (pages 179-194) DOI: 10.22203/eCM.v026a13 ISSN 1473-2262

SOLID FREEFORM-FABRICATED SCAFFOLDS DESIGNED TO CARRY MULTICELLULAR MESENCHYMAL STEM CELL SPHEROIDS FOR CARTILAGE REGENERATION

G.-S. Huang[1], C.-S. Tseng[2], B. Linju Yen[3,4], L.-G. Dai[5], P.-S. Hsieh[1] and S.-h. Hsu[1,6]

[1]Institute of Polymer Science and Engineering, National Taiwan University, Taipei, Taiwan
[2]Department of Mechanical Engineering, National Central University, Taoyuan, Taiwan
[3]Institute of Cellular and System Medicine, National Health Research Institutes, Miaoli, Taiwan
[4]Department of Obstetrics/Gynecology, Cathay General Hospital Shiji, New Taipei City, Taiwan
[5]Department of Orthopedics, Kuang Tien General Hospital, Taichung, Taiwan
[6]Research Center for Developmental Biology and Regenerative Medicine, National Taiwan University, Taipei, Taiwan

Abstract

Three-dimensional (3D) cellular spheroids have recently emerged as a new trend to replace suspended single cells in modern cell-based therapies because of their greater regeneration capacities *in vitro*. They may lose the 3D structure during a change of microenvironment, which poses challenges to their translation *in vivo*. Besides, the conventional microporous scaffolds may have difficulty in accommodating these relatively large spheroids. Here we revealed a novel design of microenvironment for delivering and sustaining the 3D spheroids. Biodegradable scaffolds with macroporosity to accommodate mesenchymal stem cell (MSC) spheroids were made by solid freeform fabrication (SFF) from the solution of poly(D,L-lactide-co-glycolide). Their internal surface was modified with chitosan following air plasma treatment in order to preserve the morphology of the spheroids. It was demonstrated that human MSC spheroids loaded in SFF scaffolds produced a significantly larger amount of cartilage-associated extracellular matrix *in vitro* and in NOD/SCID mice compared to single cells in the same scaffolds. Implantation of MSC spheroid-loaded scaffolds into the chondral defects of rabbit knees showed superior cartilage regeneration. This study establishes new perspectives in designing the spheroid-sustaining microenvironment within a tissue engineering scaffold for *in vivo* applications.

Keywords: Solid freeform fabrication; scaffolds; mesenchymal stem cell spheroids; chitosan; cartilage regeneration.

*Address for correspondence:
Shan-hui Hsu
Institute of Polymer Science and Engineering
National Taiwan University
No. 1, Sec. 4 Roosevelt Road,
Taipei 10617, Taiwan, R.O.C.
Telephone Number: 886-2-3366-5313
FAX Number: 886-2-3366-5237
E-mail: shhsu@ntu.edu.tw

Introduction

Stem cells are multipotent cells that can differentiate into different lineages and expand while maintaining their undifferentiated state (self-renewal). Mesenchymal stem cells (MSCs) show adhesion to tissue culture polystyrene (TCPS) dish with fibroblast-like cell morphology and are normally characterised with their specific lack of haematopoietic and endothelial markers but with variable expressions of several other surface antigens (e.g. CD73, CD90, and CD105). A three-dimensional (3D) culture environment is generally considered more favourable than 2D monolayer culture. Various culture systems have emerged lately to generate 3D multicellular spheroids from MSCs, such as suspension, hanging drop, micropatterned substrates, and non-adherent surface (Potapova *et al.*, 2007; Wang *et al.*, 2009; Bhang *et al.*, 2011; Su *et al.*, 2013). MSC spheroids formed on micropatterned substrates had higher efficiency of osteogenic and adipogenic differentiations (Wang *et al.*, 2009). Those generated from hanging drop or suspension had better anti-inflammatory property (Bartosh *et al.*, 2010; Ylostalo *et al.*, 2012) and angiogenesis capacity (Bhang *et al.*, 2011). A novel method has been established recently to generate MSC spheroids on chitosan-based substrates such as chitosan membranes (CS) (Hsu *et al.*, 2012c) or hyaluronan-modified chitosan membranes (CS-HA) (Huang *et al.*, 2011). MSCs grown on these substrates were self-assembled into 3D cellular spheroids that kept migrating on the substrates. The self-renewal property and chondrogenic differentiation potential were significantly enhanced in these substrate-derived MSC spheroids (Huang *et al.*, 2011; Hsu *et al.*, 2012a). Although MSC spheroids are considered superior to single suspended cells in general, the delivery of relatively bulky spheroids without losing their 3D structure is a challenging task. Moreover, no study has ever followed if these MSC spheroids can truly maintain their 3D morphology upon a change of microenvironment.

Scaffolds are a key component in cartilage tissue engineering, which provide a suitable microenvironment for cell development. Biodegradable scaffolds have been fabricated by a variety of methods, e.g., solvent casting/particulate leaching, phase separation, freeze-drying, and fibre bonding (O'Shea and Miao, 2008). However, the pore size and porosity of these scaffolds are difficult to control. Solid freeform fabrication (SFF) methods are a category

of techniques for reproducibly controlling the internal pore size (50-800 μm), porosity, pore interconnectivity, and mechanical performance of tissue engineering scaffolds (Kim *et al.*, 2009; Zorlutuna *et al.*, 2012). 3D porous scaffolds can be made from polymer solutions in precise size and shape by one of the SFF techniques, i.e. liquid frozen deposition manufacturing (LFDM). These scaffolds consist of regularly stacking fibres. SFF/LFDM scaffolds fabricated from poly(D,L-lactide-co-glycolide) (PLGA) solution were found to support the growth of chondrocytes and allow them to deposit the extracellular matrix in the large open space among the stacking fibres (i.e. macroporosity) (Yen *et al.*, 2009). It is rational to assume that SFF scaffolds with the macroporosity in contrast to microporosity of the traditional scaffolds may be particularly suitable for delivering the relatively large MSC spheroids for cell therapy.

So far, there is no investigation on if any microenvironment, material, or scaffold may adopt cellular spheroids and maintain their 3D multicellular state for a long duration. The subject, however, is crucial for clinical and translational research. Our hypothesis is that spheroids are superior to dispersed single cells in cartilage regeneration, but the spheroid morphology should be maintained when cells are seeded in a scaffold. In this contribution, we designed scaffolds suitable for seeding 3D spheroids and maintaining their morphology, and we tested their efficacy *in vitro* and *in vivo*. First, biodegradable scaffolds were fabricated by the SFF technique and by surface modification. Cellular spheroids were derived from the self-assembly of human placenta MSCs grown on chitosan-based substrates. We demonstrate that SFF scaffolds, when properly designed, can house 3D cellular spheroids and maintain their advantages for cartilage regeneration *in vivo*. This work lays the foundation for new perspectives on designing a microenvironment to sustain the spheroids in a next-generation tissue-engineering scaffold.

Materials and Methods

Fabrication of SFF scaffolds

PLGA precision scaffolds were fabricated by an SFF system (LFDM). The self-developed injection system integrated a personal computer and an x-y-z motion platform with a condenser. The computer was used for design of scaffold models, planning of manufacturing paths, and motion control of the platform. The biomedical-grade polymer, PLGA 50:50 (inherent viscosity = 0.88 dl/g; Purac, Gorinchem, The Netherlands) dissolved in 1,4-dioxane (Tedia, Fairfield, OH, USA) (20 % w/v), was filled into a trough and injected through the nozzle. The temperature of the platform and the frozen rate of the feeding solution were optimised to fabricate the well-defined stacking layers and structures. The patterns of the scaffolds could be designed by adjusting the following parameters: fibre stack angles, nozzle aperture (Φ_n), and centre-to-centre distance between adjacent fibres (d_h). The structure of scaffolds was examined by scanning electron microscopy (SEM). The compression modulus was determined by a dynamic mechanical analyser (DMA Q800, TA) at 37 °C and in 1 Hz. Scaffolds of any size and shape could be manufactured. The dimension and shape (disc cylinders 6.5 mm in diameter and 2.5 mm in thickness) were selected for experimental purposes.

Scaffolds produced were further coated with chitosan. Chitosan powder (Sigma-Aldrich, St. Louis, MO, USA) molecular weight 510 kDa, and degree of deacetylation 77 %) was dissolved in 1 % acetic acid to obtain a 1 % chitosan solution. Before coating, PLGA scaffolds were activated by air plasma generated from an Openair® plasma system (RD1004, Steinhagen, Germany). Air plasma (1000 W) was generated and ejected from a rotating nozzle with 0.5 cm diameter. The plasma source was the compressed filtered/purified dried air (21 % oxygen and 79 % nitrogen, pressure 2.5 kg/cm^2, temperature 26 °C). The scaffolds were placed at a distance of 10 mm from the plasma-ejecting nozzle. The scan speed of the nozzle was 6.4 m/min. The scaffolds were scanned twice, once on the top and once on the bottom, placed immediately in the chitosan solution (5 μL) for 120 min at 37 °C, and washed extensively by distilled water. The chitosan modified precision scaffolds were abbreviated as "PLGA-CS" SFF scaffolds. The modified scaffolds were stained with 2 % aqueous solution of Alizarin red S (Sigma-Aldrich).

Preparation of PLGA and PLGA-CS membranes

PLGA 50:50 was dissolved in 1,4-dioxane at a final concentration of 20 % (w/v). The solution was cast on 1.5 cm-diameter coverslip glass and evaporated for 72 h. PLGA membranes were further modified by chitosan using air plasma treatment ("PLGA-CS" membranes). The condition of air plasma for surface modification followed that previously described for scaffolds but with only one scan on the top surface of the membranes. After plasma treatment, 300 μL of the chitosan solution was coated on the membranes, incubated for 120 min at 37 °C, and washed by distilled water. The surface chemical composition was analysed by the attenuated total reflection infrared (ATR-IR) spectroscopy.

Isolation and culture of human placenta-derived MSCs

Human placenta-derived MSCs were obtained with approval from the Institutional Review Board (#IRB CT9607). Cells were isolated based on a previous protocol (Yen *et al.*, 2005). The donor ages were 28-, 23- and 36-year-old healthy women. The culture medium was Dulbecco's modified Eagle's medium (DMEM)-low glucose (Gibco) supplemented by 10 % (v/v) foetal bovine serum (FBS, HyClone/Thermo Scientific, Waltham, MA, USA), 1 % antibiotics (penicillin-streptomycin, Gibco, Invitrogen/Life Technologies, Carlsbad, CA, USA), and 10 mg/L L-glutamine. The medium was replaced twice every week. The experiments were repeated on cells of 7-10 passages (considered as early passages) (Ho *et al*., 2013) from at least three different donors. The expression of surface markers (genuineness of MSCs) was characterised by flow cytometry (positive for CD29, CD44, CD73, CD90 and D105; and negative for CD31, CD34 and CD45) (Huang *et al*., 2011).

Preparation of self-assembled MSC spheroids based on CS and CS-HA (i.e., CS derived spheroids and CS-HA derived spheroids)

MSC spheroids were generated from cell self-assembly on two types of chitosan-based membranes. The aforementioned chitosan solution (300 µL) was coated on 1.5 cm-diameter coverslip glass placed in a Petri dish, where membranes formed after solvent evaporation (Hsu *et al.*, 2012c). For the preparation of CS-HA membranes, 300 µL solution of hyaluronan (HA sodium salt, SciVision Biotech, Kaohsiung, Taiwan; molecular weight ~2,500 kDa) was added on each chitosan-coated coverslip glass so the amount of HA was 0.5 mg/cm^2 (Huang *et al.*, 2011). The chitosan membranes and those modified by HA were each abbreviated as "CS" and "CS-HA". Human placenta-derived MSCs ($3 \cdot 10^4$ cells/cm^2) were seeded on each CS or CS-HA membrane in 24-well tissue culture plates. The formation of spheroids was verified at 72 h by a phase contrast microscope. For cell tracking, MSCs prior to seeding were labelled in red fluorescence with a fluorescent cell linker kit PKH26 ($4 \cdot 10^{-6}$ M; Sigma-Aldrich) in the dilution buffer for 5 min. The self-assembled 3D spheroids were detached from CS or CS-HA membranes by placing the culture plates on a shaker in laminar cabinet and shaking for 5 min. MSC spheroids derived from CS membranes were referred to as "CS derived spheroids" while those derived from CS-HA membranes were referred to as "CS-HA derived spheroids".

Behaviour of MSC spheroids replated on PLGA and PLGA-CS membranes

MSC spheroids (containing ~$5 \cdot 10^4$ MSCs) were harvested at 72 h from CS or CS-HA membranes (i.e., the pristine spheroids). They were immediately replated on PLGA and PLGA-CS membranes placed in 24-well tissue culture plates, as well as CS membranes and blank wells (TCPS) serving as controls. The gene expression levels of cytokines BMP-2 and TGF-β3 were analysed by real-time polymerase chain reaction (RT-PCR) using a Chromo 4 PTC200 Thermal Cycler (MJ Research, St. Bruno, Quebec, Canada) and the DyNAmo Flash SYBR Green qPCR Kit (Finnzymes, Espoo, Finland). The expression levels were normalised to GAPDH. The protein expression of N-cadherin was analysed by Western blots using primary antibodies for N-cadherin and GAPDH (Epitomics/Abcam, Cambridge, UK). Data were obtained at 3 days and weekly after replating the pristine spheroids. For chondrogenic induction, the basal medium was replaced with the chondrogenic induction medium after the pristine MSC spheroids were replated on each material (PLGA, PLGA-CS, CS, and TCPS) for a week. The induction medium was DMEM-high glucose (Gibco) containing 10 % FBS, 10 ng/mL TGF-β3 (CytoLab/Peprotech, Rehovot, Israel), 0.1 µM dexamethasome, 50 µg/mL ascorbate-2-phosphate, 40 µg/mL L-proline, 1 % insulin-transferrin-selenium (ITS)-premix 100× and 1 % antibiotics. The induction medium was changed twice a week. After induction for 2 or 4 weeks (i.e., a total of 3 or 5 weeks after replating), the expression of chondrogenesis representative genes, Sox9, aggrecan (Aggr), and collagen type II (Col II) were analysed by the real-time RT-PCR. The primer sequences are listed in Table 1.

Cell migration assay

MSC spheroids (containing ~$5 \cdot 10^4$ MSCs) were harvested at 72 h from CS-HA membranes (the pristine spheroids). They were immediately replated on CS, PLGA, and PLGA-CS membranes placed in the lower chamber of a transwell (fit in a 24 well plate). The control groups included blank wells (TCPS) with spheroids and wells without any replated spheroids. After cells in the lower chamber were incubated for 3 days, they were analysed for SDF-1 gene expression. In additional groups, $1 \cdot 10^4$ MSCs (PKH26 labelled) were further added in the upper chamber. After another 24 h, the upper surface of the transwell filters was scraped free of cells and the cell number in the lower surface was counted (i.e., the number of labelled cells migrated from the upper to the lower). Data were confirmed in three independent experiments. To verify the driving force of migration, MSCs were pre-incubated with 200 ng/mL AMD3100 (a specific antagonist of SDF-1, Sigma-Aldrich) for 30 min at 37 °C in some experimental

Table 1. The primer sequences used for real-time RT-PCR analyses.

Genes	Primer sequences	Primer annealing temperature (°C)
BMP-2	5'-ACAGGCTGGACAGAGGAGAA	60
	3'-GGGCAAGGGCAAGGGGAAGA	
TGF-β3	5'-CTGCTGCTGTGAGGGATGTTAT	58
	3'-GGTCGAGGCTTCTGCTTATTTC	
SDF-1	5'- GAAGTGGAGCCATAGTAATGCC	58
	3'- TCCAAGTGGAAAAATACACCG	
Sox9	5'-CTAAGAGGCATCCAAACAACACA	56
	3'-CCCTCGCTGCTAAAGTGTAATAA	
Aggr	5'-TCAATAGGCAAGCGAAACCC	60
	3'-GAGTGCTGGAGATAAACCCTTCA	
Col II	5'-TACCTCAGCCTCCAGCAGAT	58
	3'-CGTCACACCATTGCTATTCTT	
GAPDH	5'-AATGTGTCCGTCGTGGATCTGA	56
	3'-AGTGTAGCCCAAGATGCCCTTC	

groups. To avoid the possible contribution from materials rather than cells in the lower chamber, data from materials without the replated spheroids were collected to contrast the effect.

Loading MSC spheroids into SFF scaffolds and chondrogenesis *in vitro*

$1 \cdot 10^6$ cells (in the form of single cells or spheroids) were seeded to the precision scaffolds by dropping the cell (or spheroid) suspension (50 µL) embedded with different densities of HA solution (0.6 mg/mL, 3 mg/mL, and 15 mg/mL) on the top of the SFF scaffolds. After 6 h, the seeded scaffolds were added with the culture medium. After 24 h, the seeding efficiency was determined by counting the cell number in the constructs as described later, and expressed as the percentage of the initial cells added.

To perform chondrogenic induction, the basal medium was replaced with the chondrogenic induction medium after single cells or spheroids were seeded in SFF scaffolds for a week. The induction medium was changed twice a week. After induction for 4 weeks, the constructs were subjected for gene analysis, histological examinations, or biochemical assays described later.

Neocartilage formation in mice

Scaffolds seeded with MSC single cells or spheroids were cultured in basal medium for the first week. Chondrogenic induction medium was then added to induce *in vitro* chondrogenesis of the seeded cells for a week (2 weeks from initial seeding) before implantation. All protocols involving the use of animals in this study were approved by the Experimental Animal Committee of the university. Ten nude mice were used in total, where samples were implanted on right and left subcutaneous sites. For each group, $n = 5$ Human MSC-seeded scaffolds were implanted subcutaneously into the female eight-week-old NOD/SCID mice for 4 weeks *in vivo*. Four animals were used in each group. The explanted constructs were subjected to histological or biochemical analyses.

Cartilage regeneration in rabbit joint cartilage defects

Rabbit MSCs were isolated from the adipose tissue from mature adult New Zealand white rabbits (weighing 3-3.5 kg). MSCs were incubated in basal medium. Six rabbits were used in total, where samples were implanted in right and left hind legs. For each group, $n = 4$. Allogenic cells of the third passage were used in animal implantation. MSC spheroids were harvested after cell culture on CS-HA membranes for 72 h. SFF PLGA-CS scaffolds loaded with rabbit CS-HA derived MSC spheroids were further incubated in the basal medium for another 72 h before implantation. A full-thickness cylindrical cartilage defect of 3 mm in diameter and 3 mm in depth was created in the patellar groove of the experimental rabbit using a stainless steel drill. MSCs ($\sim 1 \cdot 10^6$) in the form of single cells or spheroids were loaded in each scaffold. After being pre-cultured *in vitro*, the single cell-loaded or spheroid-loaded scaffolds were implanted into the defect for one month *in vivo*. Four animals were used for each type of the constructs. The explanted constructs were subjected to histological examinations.

Biochemical assays and histological examinations of the neocartilage

Constructs were washed in phosphate buffered saline and freeze-dried overnight. They were digested in papain (Sigma) solution at 60 °C for 24 h. Cell number was analysed after reaction with 0.1 µg/mL Hoechst 33528 dye (Sigma-Aldrich) (Yen *et al.*, 2009). The glycosaminoglycan (GAG) content was quantified by the dimethylmethylene blue (DMMB) method (Yen *et al.*, 2009). Type II collagen contents of the constructs were quantified by an ELISA assay kit (ASB-5000-EX, Rheumera™) after digestion with pepsin at 25 °C. Histological samples were fixed in 4 % paraformaldehyde at 4 °C, embedded, and sectioned to 10 µm. The sections were stained with haematoxylin & eosin (H&E) or Safranin O, or immunostained with anti type II collagen (Lab Vision/Neomarkers, Freemont, CA, USA). Cell nuclei were stained by 4',6-diamidino-2-phenylindole (DAPI).

Statistical analysis

Numerical values were expressed as the mean ± standard deviation. For each type of experiment, three similar experiments were performed independently. Reproducibility was confirmed for cells from at least three different healthy donors. Statistical differences among the experimental groups were evaluated by analysis of variance followed by Student's *t*-test. *p*-values <0.05 were considered statistically significant. Data from different donors were not mixed; therefore, *p*-values <0.01 should be more than sufficient.

Results

Preparation of SFF Scaffolds

Macroporous PLGA scaffolds were designed and made by SFF/LFDM procedures. With a three-axis motion controlled system, 20 % PLGA solution (in 1,4-dioxane) was dispensed through a micro-nozzle coupled to a low temperature platform, as shown in Fig. 1a. The polymer solution was frozen, stacked into a multilayer scaffold, and freeze-dried. SEM images (Fig. 1b) confirmed the well-defined layer-by-layer structures that were generally matched to those of the original designs. Scaffolds optimised for the present study were disc cylinders 6.5 mm in diameter and 2.5 mm in thickness. The patterns of scaffolds were defined by the following parameters: stack angles, 4D (0°/90°/45°/135°); nozzle aperture (Φ_n), 0.2 mm; and centre-to-centre distance between adjacent fibres (d_h), 0.7-1.0 mm, as shown in the figure. Each stacking fibre was microporous (pore size ~1 µm). The dynamic compression modulus (E') of the scaffold was ~0.5 MPa, close to that of normal cartilage (Yen *et al.*, 2009).

PLGA membranes and PLGA SFF scaffolds were surface-modified with chitosan after air plasma treatment (abbreviated as "PLGA-CS", Fig. 2a). ATR-IR spectra

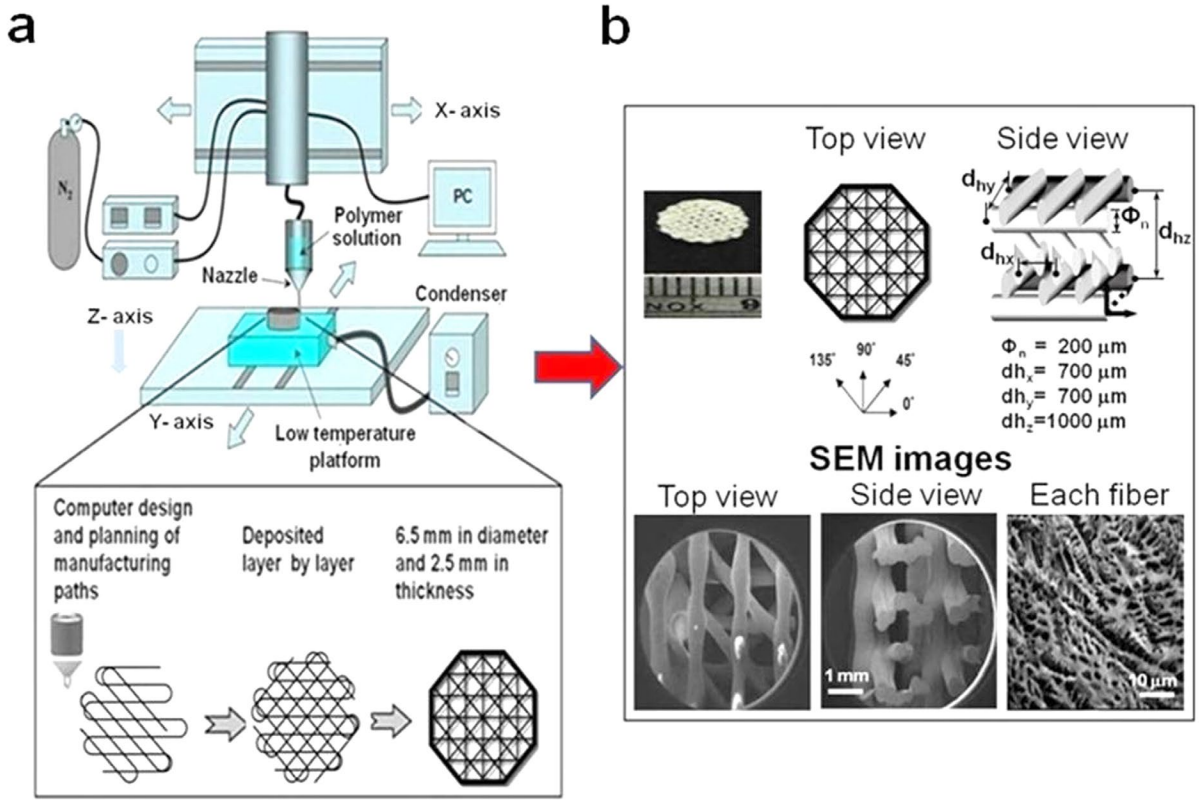

Fig. 1. Fabrication of the SFF scaffolds by LFDM processes. **(a)** Schematics for fabrication of SFF scaffolds from the PLGA polymer solution. Parameters of SFF scaffolds: stack angle, nozzle aperture (Φ_n), and interval between adjacent fibres (d_h). **(b)** SEM images showing the top and lateral views of the scaffold (macroporosity), as well as the microporous structure in each stacking fibre.

confirmed the presence of chitosan (–NH peak at 1582 cm^{-1} and C-C backbone in-plane peak at 1050 cm^{-1}) (Nosal *et al.*, 2005) on the surface of PLGA-CS membranes (Fig. 2b). PLGA-CS scaffolds were stained red with Alizarin red S, a dye that binds to chitosan (Fig. 2c), to demonstrate the chitosan-modified surface (*vs.* unmodified control).

Generation and maintenance of the self-assembled human MSC spheroids

Chitosan-based substrates (CS and CS-HA membranes) were utilised for forming MSC spheroids (Fig. 3a). MSCs isolated from human placenta were self-assembled into 3D spheroids in 72 h. The average size of spheroids derived on CS was 60 ± 27 μm and that on CS-HA was 100 ± 20 μm. When these MSC spheroids were relocated to PLGA membranes or TCPS for 3 days, the spheroid state was not well maintained; while placing spheroids on CS or PLGA-CS membranes could preserve the morphology of the spheroids (Fig. 3a). The expression level of N-cadherin, a cell-cell adhesion protein that indicates the degree of cell-cell interaction, was analysed. For the pristine MSC spheroids (self-assembled at 3 days) and those replated on CS, TCPS, PLGA or PLGA-CS membranes for 3, 7 and 14 days, the expression levels of N-cadherin are shown in Fig. 3b and Fig. 3c. The expression level of N-cadherin for the pristine MSC spheroids derived on CS or CS-HA was significantly higher than that of MSCs on TCPS ($p = 0.0072$ and $p = 0.0051$ for each). The pristine CS-HA derived spheroids had the greatest N-cadherin expression. After replating, the expression level of N-cadherin for spheroids replated on CS or PLGA-CS was sustained and remained relatively stable during the 2-week period. On the other hand, the expression of N-cadherin declined significantly when spheroids were replated on PLGA or TCPS. Based on the analysis, substrate materials that sustain the cell-cell adhesion (N-cadherin) can keep the morphology of the 3D spheroids properly.

The chondrogenic differentiation potential of replated MSC spheroids is shown in Fig. 3d. The expression of chondrogenesis representative genes, including Sox9, Aggr, and Col II, in MSC spheroids replated on PLGA-CS or CS membranes markedly increased and was significantly greater than that in spheroids replated on PLGA membranes or TCPS after 2 weeks of induction (data not shown). The expression of these genes on PLGA-CS or on CS was further upregulated at 4 weeks, particularly for Aggr and Col II of the replated CS-HA derived spheroids (Fig. 3d). Therefore, surface modification by chitosan is essential for PLGA substrates to maintain the 3D spheroid structure and chondrogenic capacity of MSCs.

The gene expression level of cytokines BMP-2 and TGF-β3 for the pristine MSC spheroids was significantly higher (each about 3.6- and 2.4-fold higher) than that of MSCs on TCPS (Fig. 4). The gene expression level of both cytokines declined significantly when spheroids were replated on PLGA membranes or TCPS. These data further support the necessity of preserving 3D spheroid morphology for beneficial MSC properties.

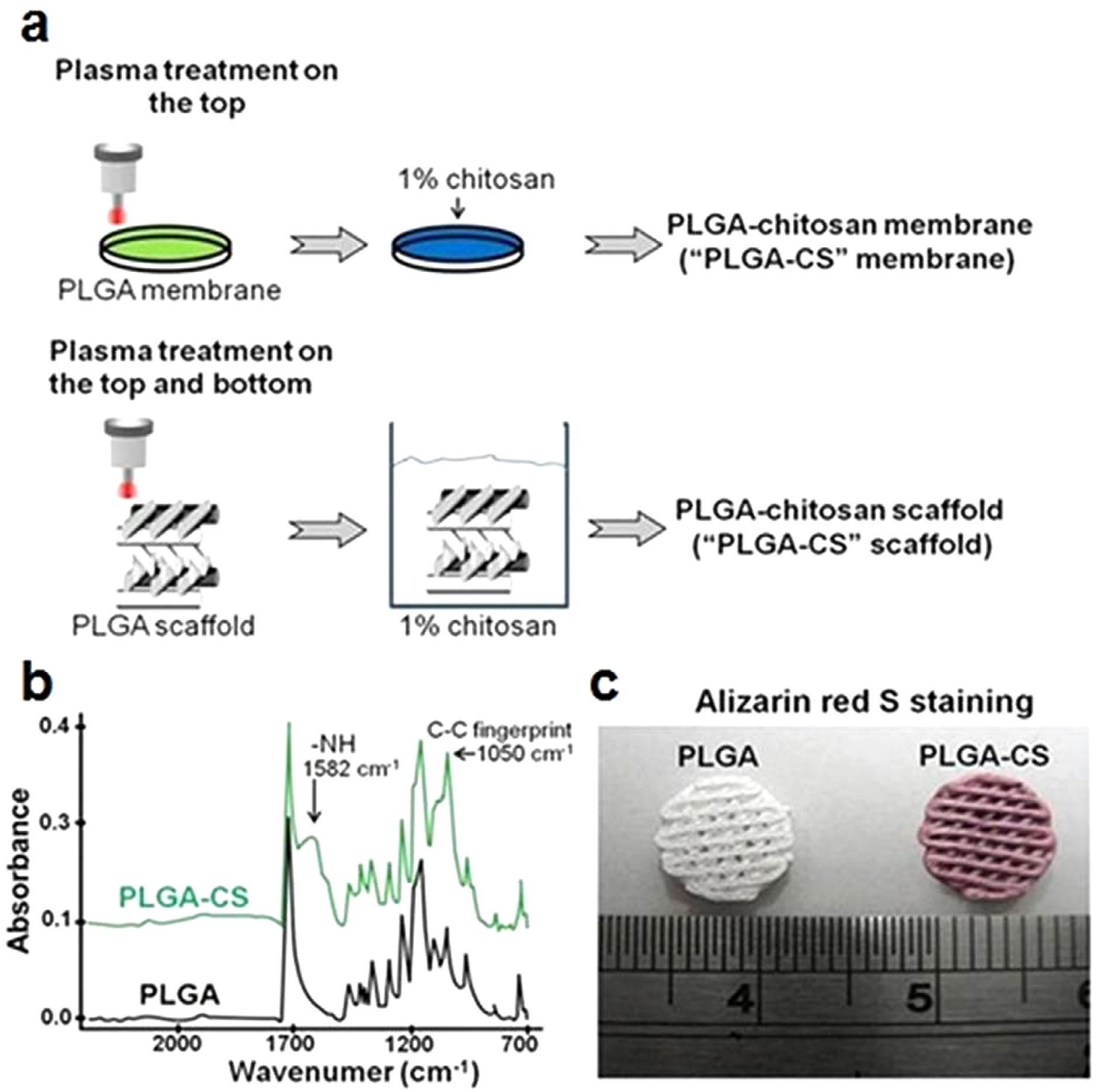

Fig. 2. Surface modification by chitosan. **(a)** PLGA membranes or PLGA SFF scaffolds were surface-modified by chitosan following air plasma treatment (Openair® air plasma system). **(b)** ATR-IR spectra of PLGA-CS membranes confirming the surface modification of PLGA by chitosan. The absorption peak at 1582 cm^{-1} was attributed to –NH (amide II) of chitosan while that at 1050 cm^{-1} was assigned to the C-C fingerprint (backbone in-plane orientation) of chitosan. **(c)** The chitosan-coated PLGA scaffold (PLGA-CS SFF scaffold) stained with Alizarin red S to demonstrate the chitosan coating on the scaffold surface.

The chemotactic effect of the replated spheroids *in vitro* is shown in Fig. 5. MSC spheroids replated on CS or PLGA-CS membranes showed a greater SDF-1 gene expression levels at 1 and 3 days (Fig. 5a; $p = 0.0062$ and 0.0055 for CS *vs.* TCPS at 1 day and 3 days; $p = 0.0083$ and 0.0089 for PLGA-CS *vs.* TCPS at 1 day and 3 days). Besides, the number of recruited MSCs induced by MSC spheroids replated on CS or PLGA-CS membranes was significantly greater *vs.* those replated on PLGA or TCPS ($p = 0.0045$ and 0.0048 for CS *vs.* PLGA and CS *vs.* TCPS; $p = 0.0061$ and 0.0069 for PLGA-CS *vs.* PLGA and PLGA-CS *vs.* TCPS). When spheroids were pre-treated with the inhibitor of chemokine SDF-1, the extra recruiting ability was abolished (Fig. 5b). These data indicate that 3D MSC spheroids have a remarkable chemotactic effect.

Building the constructs from MSC spheroids and SFF scaffolds

Combining SFF scaffolds and self-assembled MSC spheroids is illustrated in Fig. 6a. To overcome the potential problem of ineffective seeding, the spheroids were suspended in HA solution prior to seeding (3 mg/mL HA being the most effective with a seeding efficiency 60-80 %. In all the following experiments, HA of 3 mg/mL was employed if the cells or spheroids were referred as embedded before seeding into scaffolds.

The seeding efficiency of MSC spheroids (*vs.* single cells) in PLGA or PLGA-CS SFF scaffolds, with or without the help from HA, are shown in Fig. 6b. In PLGA SFF scaffolds, the seeding efficiency of single cells was significantly improved after embedding in HA ($p = 0.028$);

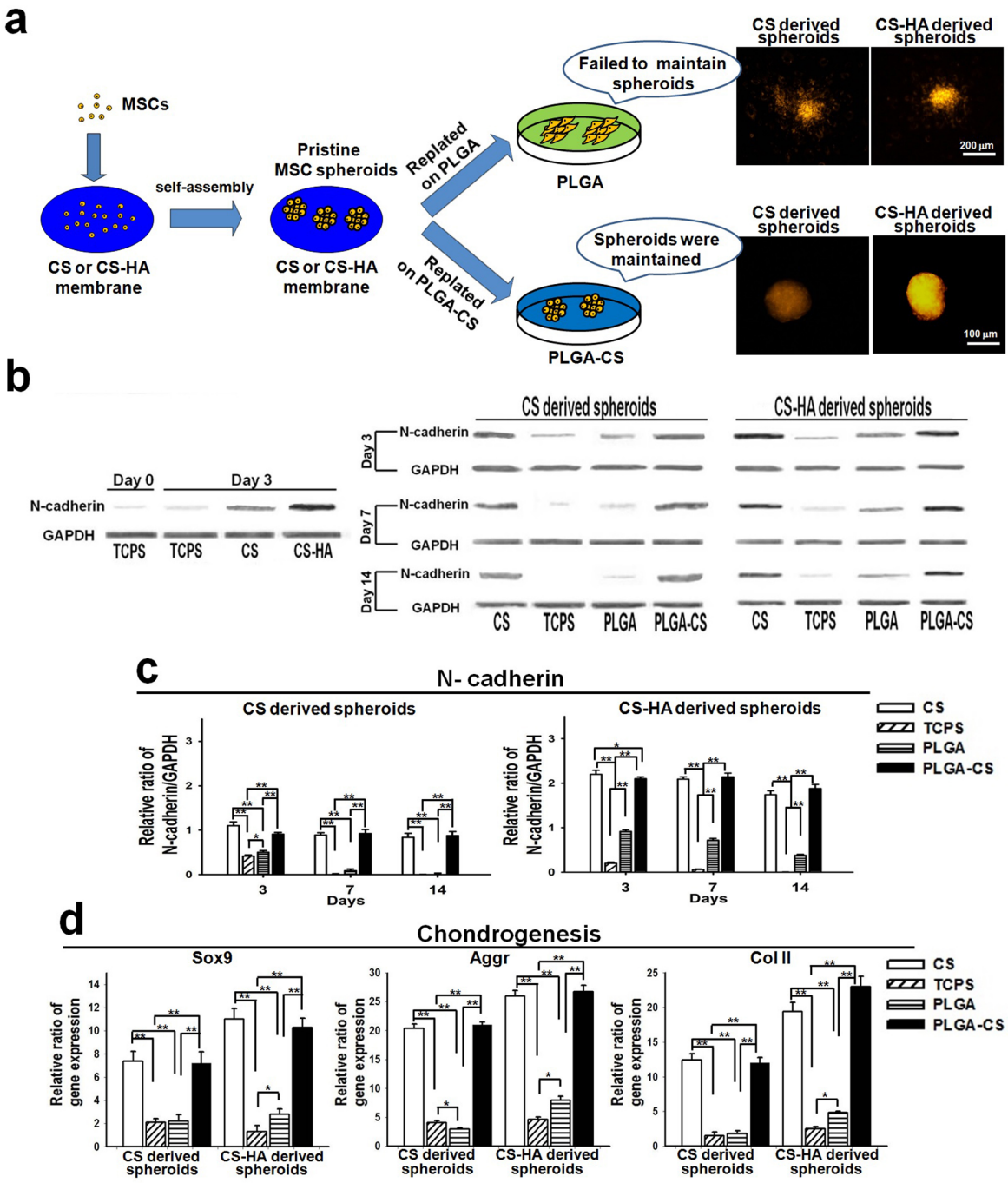

Fig. 3. The morphology, N-cadherin expression, and differentiation of MSC spheroids replated on PLGA or PLGA-CS membranes. **(a)** Schematics showing the self-assembly of MSC spheroids on CS or CS-HA membranes and the morphology of MSC spheroids after being replated on PLGA or PLGA-CS membranes for 3 days**. (b)** Western blots of N-cadherin expression for the pristine spheroids (at 3 days) as well as those replating on different materials for 3, 7 and 14 days. **(c)** Quantification of N-cadherin expression at 3, 7 and 14 days after replating. The relative ratios of N-cadherin/GAPDH were all normalised to that in the pristine CS-derived spheroids. **(d)** The expression of Sox9, Aggr, and Col II after 4 weeks of chondrogenic induction, analysed by real-time RT-PCR. The relative ratio of each gene was normalised to that in the pristine CS-derived spheroids. The induction medium was refreshed every 3 days. * refers to $p < 0.05$ among the indicated groups; ** refers to $p < 0.01$ among the indicated groups. The MSCs in the study were derived from human placenta.

while the seeding efficiency of spheroids did not change significantly after embedding in HA. In PLGA-CS SFF scaffolds, HA greatly improved the seeding efficiency of both single cells and MSC spheroids, especially for single cells and CS derived spheroids ($p = 0.0024$ and 0.0045).

The morphology of MSC spheroids or single cells grown in PLGA or PLGA-CS SFF scaffolds for 3 days is shown in Fig. 6c. PLGA-CS SFF scaffolds well sustained the spheroid morphology of the pristine spheroids. On the other hand, PLGA SFF scaffolds failed to maintain

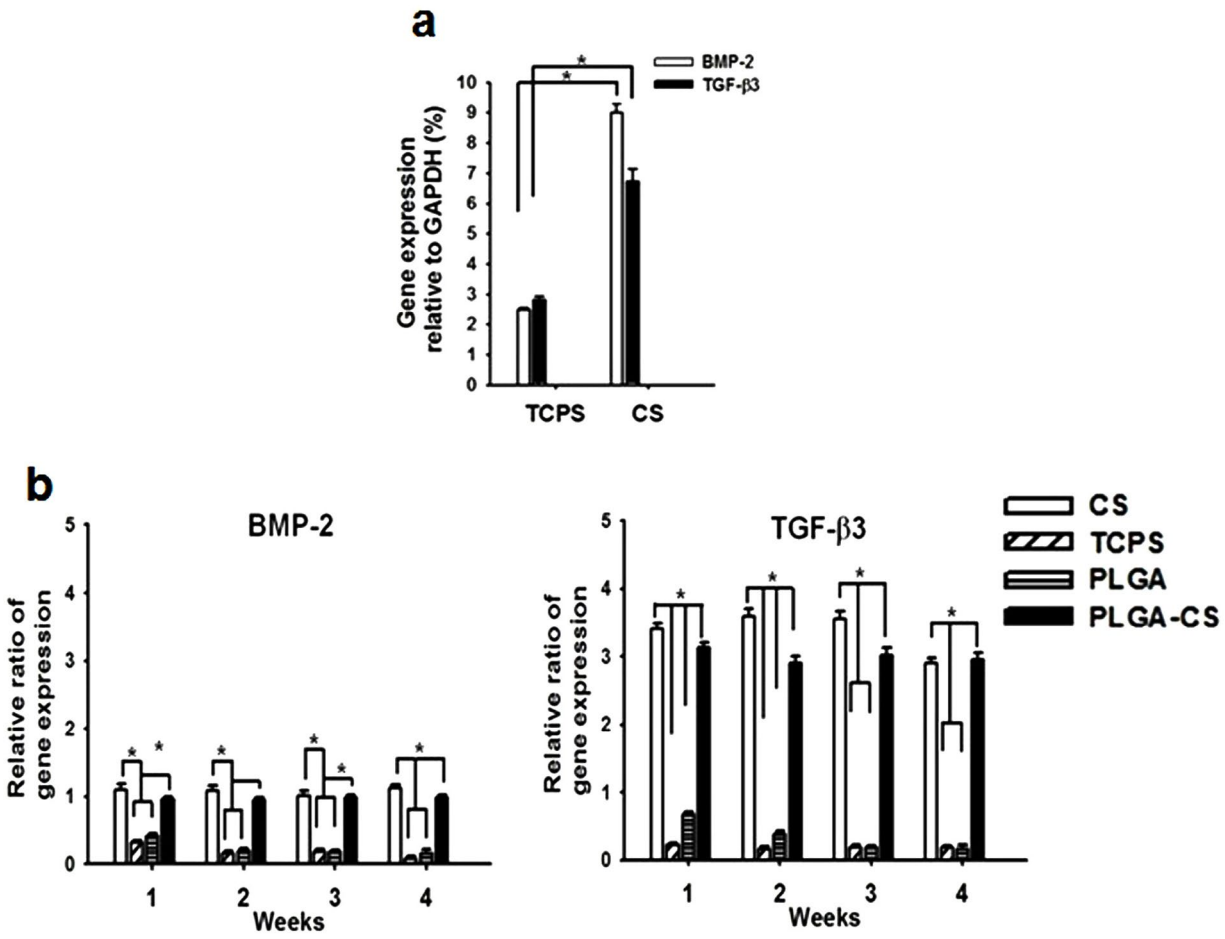

Fig. 4. The gene expression of BMP-2 and TGF-β3 for MSC spheroids and those after replating, analysed by real-time RT-PCR. **(a)** The expression for the pristine spheroids (CS derived) *vs.* single cells (TCPS). **(b)** The expression after replating on CS, TCPS, PLGA, or PLGA-CS membranes for 1, 2, 3 and 4 weeks, normalised to that of the pristine spheroids. Relative ratios larger than one indicate upregulation and those smaller than one indicate downregulation. * refers to $p < 0.05$.

the structure of the spheroids, where the spheroids were disintegrated and attached to the scaffold surface with fibroblast-like morphology. This result also indicated that HA embedment did not help sustain the morphology of the spheroids. The loss of 3D structure occurred faster for CS derived spheroids *vs.* CS-HA derived spheroids. Although embedding spheroids in HA improved the cell seeding efficiency of SFF scaffolds, it did not influence the chondrogenic differentiation (identified by the GAG content per cell) in a longer term, probably due to the solubility and limited retention time of HA in the scaffolds. As expected, the conventional microporous scaffolds had very low seeding efficiency (<10 %) for MSC spheroids, either with or without HA embedment.

The chondrogenic differentiation potential of MSC spheroids in SFF scaffolds *in vitro*

The differentiation of MSC spheroids or single cells in PLGA or PLGA-CS scaffolds after chondrogenic induction for 4 weeks *in vitro* is shown in Fig. 7a. The expression levels of chondrogenesis representative genes including Sox9, Aggr, and Col II were significantly upregulated in MSCs grown in PLGA-CS SFF scaffolds compared to those grown on PLGA SFF scaffolds. In PLGA scaffolds, the expression of all three genes in either CS-HA or CS derived spheroids was significantly greater than that in single cells. CS-HA derived spheroids had slightly higher expression of Aggr and Col II genes than CS derived spheroids, but no significant difference in Sox9 gene expression was observed between the two groups. In PLGA-CS scaffolds, the expression of all three genes was the highest in constructs loaded with CS-HA derived spheroids, followed by those with CS derived spheroids, and the lowest in those with single cells. On the other hand, Col X was significantly downregulated for MSCs grown in PLGA-CS SFF scaffolds compared to those grown in PLGA SFF scaffolds. In either type of scaffolds, the expression of Col X was lower for those loaded with spheroids and higher for those loaded with single cells.

The biochemical analysis for the neocartilage formed *in vitro* is shown in Fig. 7b. The number of cells in PLGA scaffolds increased significantly and was higher than that in PLGA-CS scaffolds. In PLGA scaffolds, cell number for the single cell-seeded group was slightly higher than that of the MSC spheroid-seeded group; while the group seeded with CS derived spheroids and that seeded with CS-HA derived spheroids had no significant difference in cell number at 4 weeks. In PLGA-CS scaffolds, cell

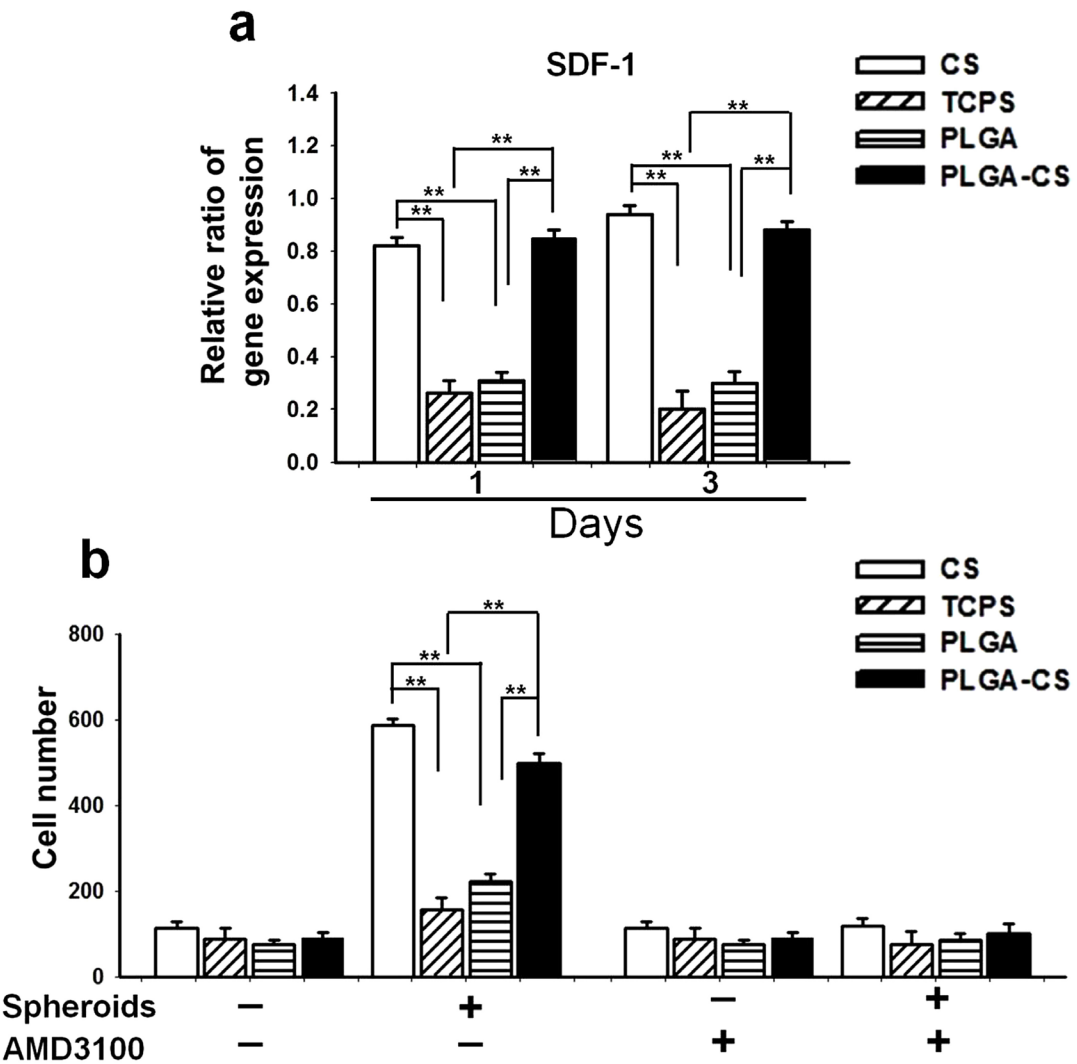

Fig. 5. The possible chemotactic effect of SDF-1 on MSC migration. MSC spheroids (CS-HA derived) replated on CS or PLGA-CS membranes, once keeping their spheroid morphology, remained to recruit more MSCs from the other side of the transwell. **(a)** The gene expression of SDF-1 for replated spheroids. **(b)** The number of recruited MSCs. * refers to $p < 0.05$ among the indicated groups; ** refers to $p < 0.01$ among the indicated groups. AMD3100 is an inhibitor of chemokine SDF-1.

number was the highest for the group seeded with CS-HA derived spheroids, followed by that with CS derived spheroids, and then that with single cells ($p = 0.041$ for CS-HA *vs.* CS derived spheroids; $p = 0.0022$ for CS-HA derived spheroids *vs.* single cells). GAG production from CS-HA derived spheroids seeded in PLGA-CS scaffolds (either on per scaffold or per cell basis) was larger than that from CS derived spheroids ($p = 0.036$), and was much larger than that from single cells. Whether in single cell- or spheroid-seeded groups, PLGA-CS scaffolds facilitated greater GAG production than PLGA scaffolds. Therefore, PLGA-CS scaffolds are good cell carriers, particularly for the spheroids.

Histological analyses are shown in Fig. 7c. Safranin O staining revealed that the expression of GAGs for MSC spheroids cultured in PLGA or PLGA-CS scaffolds was more obvious than that for single cells. In PLGA scaffolds, there was no evident difference in GAG staining between the groups of CS derived spheroids and CS-HA derived spheroids. In PLGA-CS scaffolds, the GAG staining for CS-HA derived spheroids was more obvious than that for CS derived spheroids. Due to the better GAG production and greater potential in promoting neocartilage formation *in vitro*, PLGA-CS SFF scaffolds were used in all the following *in vivo* experiments.

Neotissue formation in mice

SFF scaffolds carrying MSC spheroids were subcutaneously implanted in NOD/SCID mice for 4 weeks (Fig. 8a). Results from biochemical analyses are shown in Fig. 8b-d. Cell number in the group receiving MSC spheroid-loaded PLGA-CS SFF scaffolds was significantly greater than that in single cell-loaded or no cell-loaded (SFF only) groups ($p = 0.011$ *vs.* single cell-loaded groups; $p = 0.0089$ *vs.* no cell-loaded groups). In addition, cell number was greater in the group of CS-HA derived spheroids *vs.* CS derived spheroids ($p = 0.033$). GAG production and type II collagen (either on per scaffold or per cell basis) were the largest in constructs loaded with CS-HA derived spheroids, followed by those loaded with CS derived spheroids, and finally those with single cells.

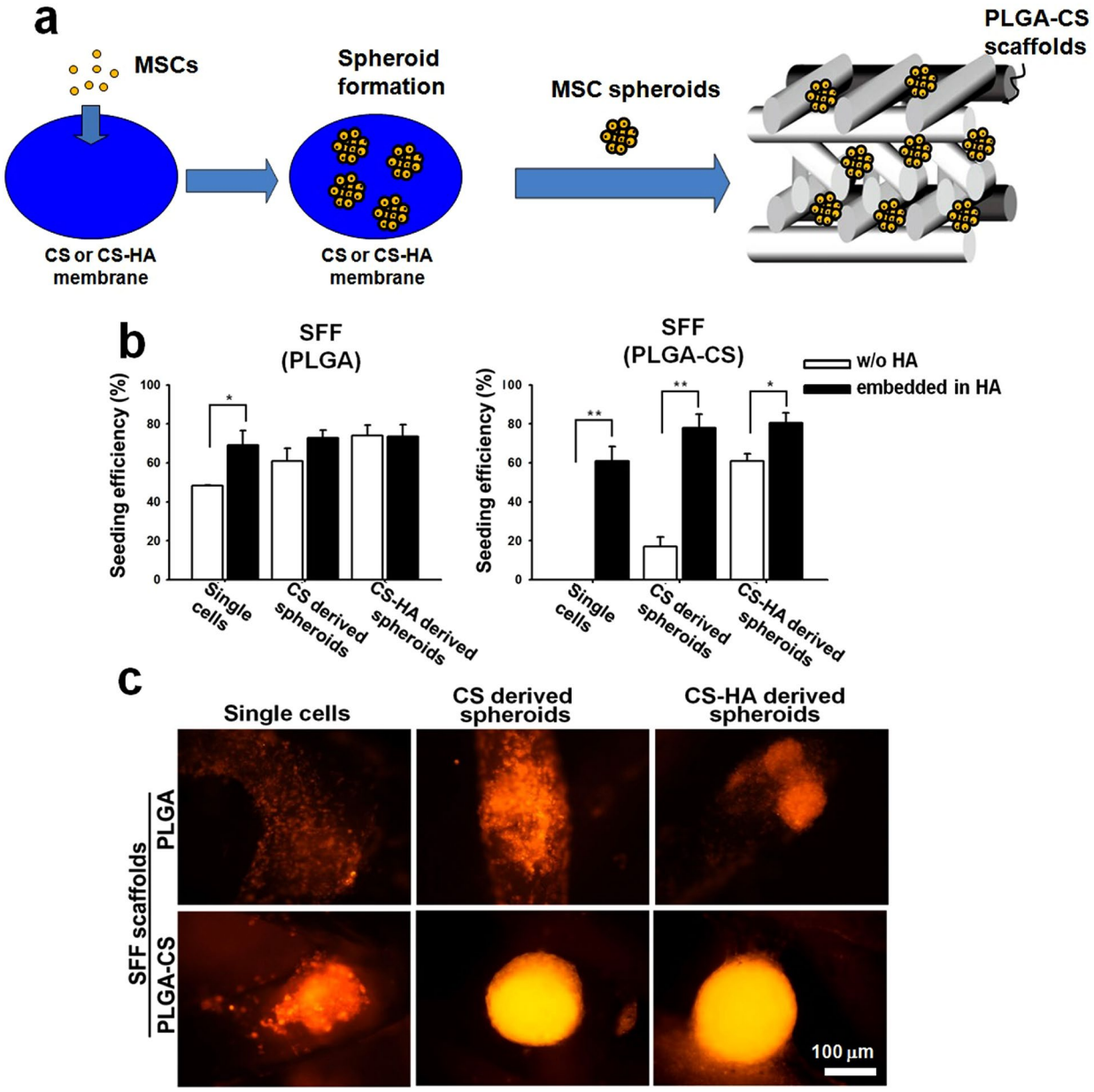

Fig. 6. Building the engineered constructs from MSC spheroids and SFF scaffolds. **(a)** A diagram showing the procedures for generating self-assembled MSC spheroids and for loading spheroids in SFF scaffolds. **(b)** The seeding efficiency of MSC spheroids in PLGA or PLGA-CS scaffolds at 1 day post seeding. **(c)** The morphology of MSC spheroids in PLGA or PLGA-CS scaffolds at 3 days post seeding. Cells were labelled with a red fluorescent cell tracker (PKH26). * refers to $p < 0.05$ among the indicated groups; ** refers to $p < 0.01$ among the indicated groups.

The histology after 4 weeks in mice is shown in Fig. 8e. Cells were labelled with a red fluorescent dye (PKH26) prior to implantation. Results from Safranin O staining and type II collagen immunofluorescence staining revealed that MSC spheroids loaded in PLGA-CS SFF scaffolds expressed more GAG and type II collagen than the single cell-loaded group or the scaffold only group. This trend was confirmed by image analysis and statistical evaluation (Fig. 8f and Fig. 8g). In the group of single cells, chondrogenesis occurred in the transplanted cells (i.e., co-localisation of dye-labelled cells with GAG/type II collagen positive cells). However, in spheroid-loaded groups, not only the loaded cells but some host cells underwent chondrogenic differentiation. Especially, CS-HA derived spheroids recruited a significant amount of host cells for neocartilage formation.

Cartilage regeneration in rabbit defects

SFF scaffolds carrying MSC spheroids were implanted in rabbits for one month (Fig. 9a). The cartilage defects receiving SFF scaffolds loaded with CS-HA derived spheroids were filled more completely with smooth white tissue compared with the single cell-seeded group. The reparative tissue was slightly different from that of the surrounding normal cartilage. The histological images are shown in Fig. 9b. H&E staining revealed more lacunae (cartilage-like tissue) in defects receiving SFF scaffolds with spheroids *vs.* those with single cells. The presence

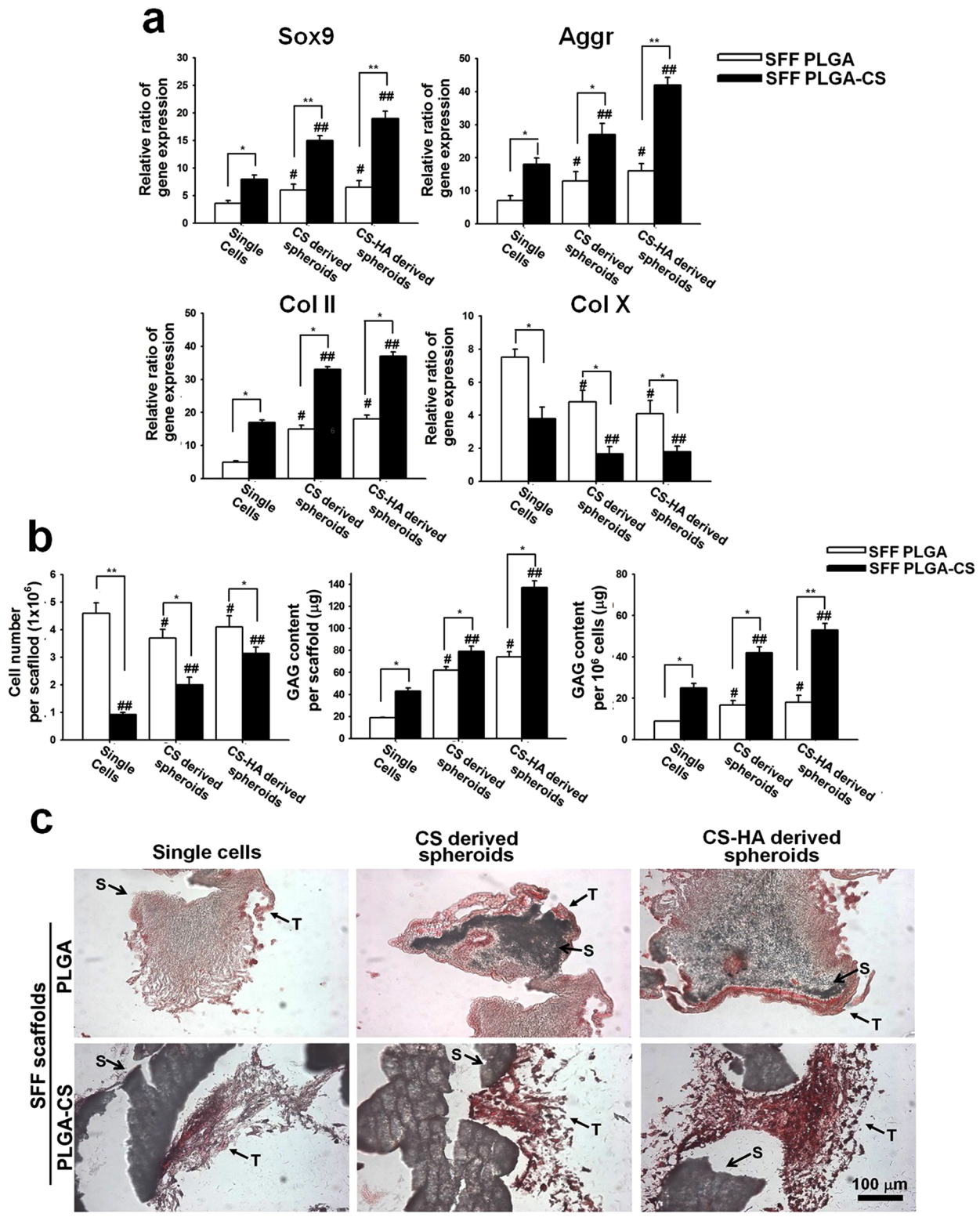

Fig. 7. Chondrogenic differentiation capacities of MSC spheroids seeded in SFF scaffolds *in vitro*. **(a)** The chondrogenesis representative genes expression (Sox9, Aggr, Col II, and Col X) after chondrogenic induction for 4 weeks. The ratio of gene expression was relative to that of the pristine single cells before seeding. **(b)** Cell number, GAG content, and the amount of GAG normalised to cell number for cells or spheroids in PLGA or PLGA-CS scaffolds after induction for 4 weeks. **(c)** The Safranin O stained histological sections after induction for 4 weeks. S: Scaffold; T: Tissue. * refers to $p < 0.05$ among the indicated groups; ** refers to $p < 0.01$ among the indicated groups.

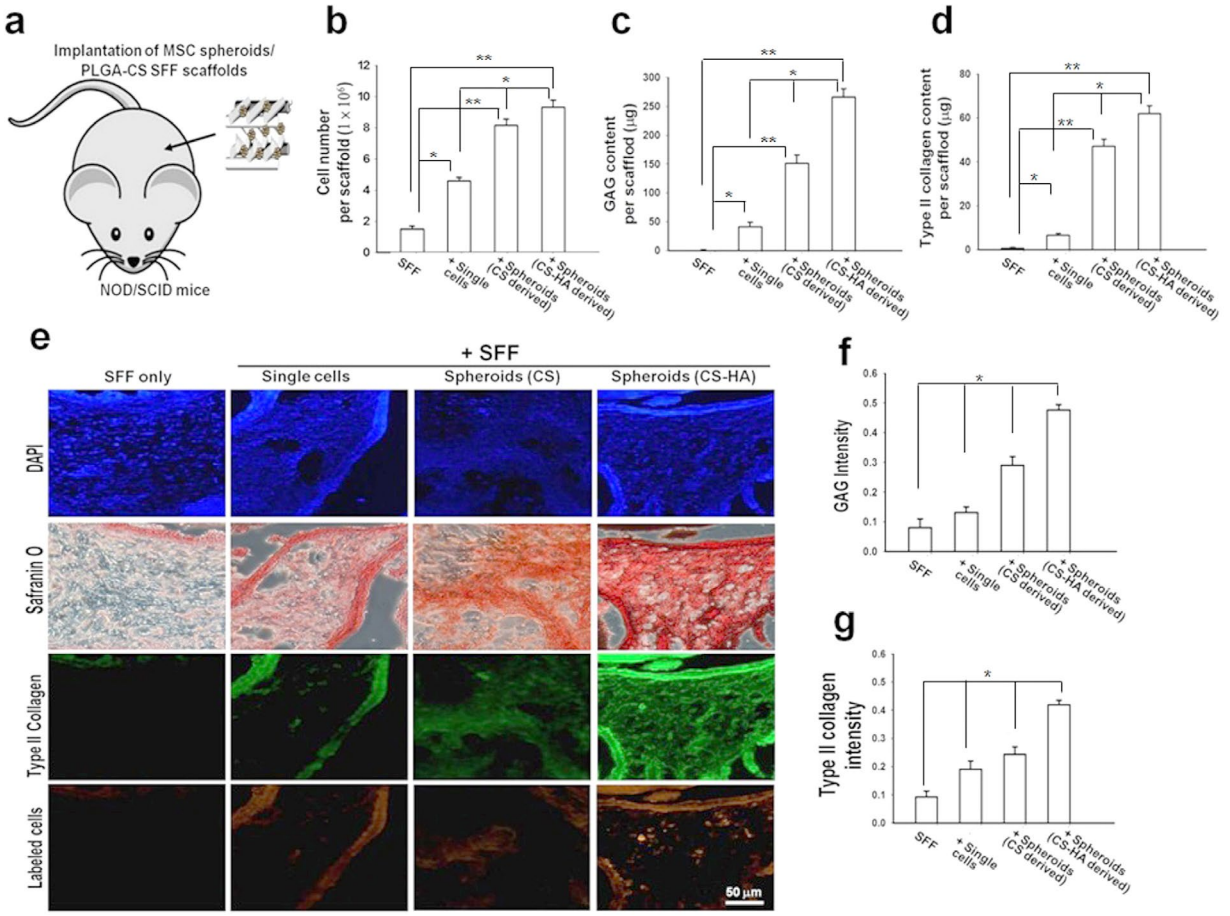

Fig. 8. Neocartilage formation ability *in vivo*. **(a)** Illustration for the subcutaneous implantation of the MSC spheroid/ SFF scaffold combined constructs in NOD/SCID mice. Analytical results for the **(b)** cell number, **(c)** GAG contents, and **(d)** type II collagen contents for MSC single cell-seeded or spheroid-loaded constructs implanted in NOD/SCID mice for 4 weeks. **(e)** The Safranin O and type II collagen-immunostained sections for MSC single cell-seeded or spheroid-loaded constructs implanted in NOD/SCID mice for 4 weeks. The intensities of GAG and type II collagen staining quantified from images are shown as **(f)** and **(g)**. The nuclei were stained by DAPI. Before animal implantation, the MSC spheroids were generated from the self-assembly of human placenta MSCs on CS or CS-HA membranes. MSCs were pre-labelled with the fluorescent cell tracker. The SFF scaffolds employed were the PLGA-CS scaffolds. * refers to $p < 0.05$; ** refers to $p < 0.01$.

of GAGs in defects implanted with spheroid-loaded SFF scaffolds was verified by the positive Safranin O staining. The group implanted with single cell-seeded SFF scaffolds was less obviously stained by Safranin O. This was confirmed by image analysis and statistical evaluation (Fig. 9c; $p = 0.029$). The cartilage defect created in the rabbit model was 3 mm deep, which was a full-thickness defect and in the close vicinity of the bone. There may be a possibility that during the surgery some underneath bone tissue was also affected, which caused the remodelling of bone in histology.

Discussion

3D spheroids of chondrocytes have been used to replace single cells in chondrocyte implantation to improve neocartilage formation (Lee *et al.*, 2011, Teixeira *et al.*, 2012). Recent *in vitro* work has suggested that 3D spheroids of MSCs may possess better differentiation capacity than single cells (Huang *et al.*, 2011; Hsu *et al.*, 2012a). MSC spheroids thus have the potential to replace MSC single-cell suspension for use in tissue engineering. Designing a proper microenvironment for these spheroids is necessary before their clinical potential can be realised (Saha *et al.*, 2007; Busscher *et al.*, 2012). For instance, cellular spheroids are much larger in size. The conventional tissue engineering scaffolds may not accommodate the MSC spheroids efficiently. One possible solution is to use the SFF scaffolds with macroporosity (Kirn *et al.*, 2010). In the current study, the polymeric scaffolds with fully interconnected macroporous structure and controlled geometry were produced by the low-temperature LFDM process. The 3D cellular spheroids were successfully seeded in the SFF/LFDM scaffolds, but failed to keep the spheroid morphology. This was attributed to the general tendency of spheroids to spread on the cell-interacting material surface (e.g., PLGA or TCPS). Modification of the cell-contacting interface by chitosan could be easily achieved after plasma penetration into the open structure

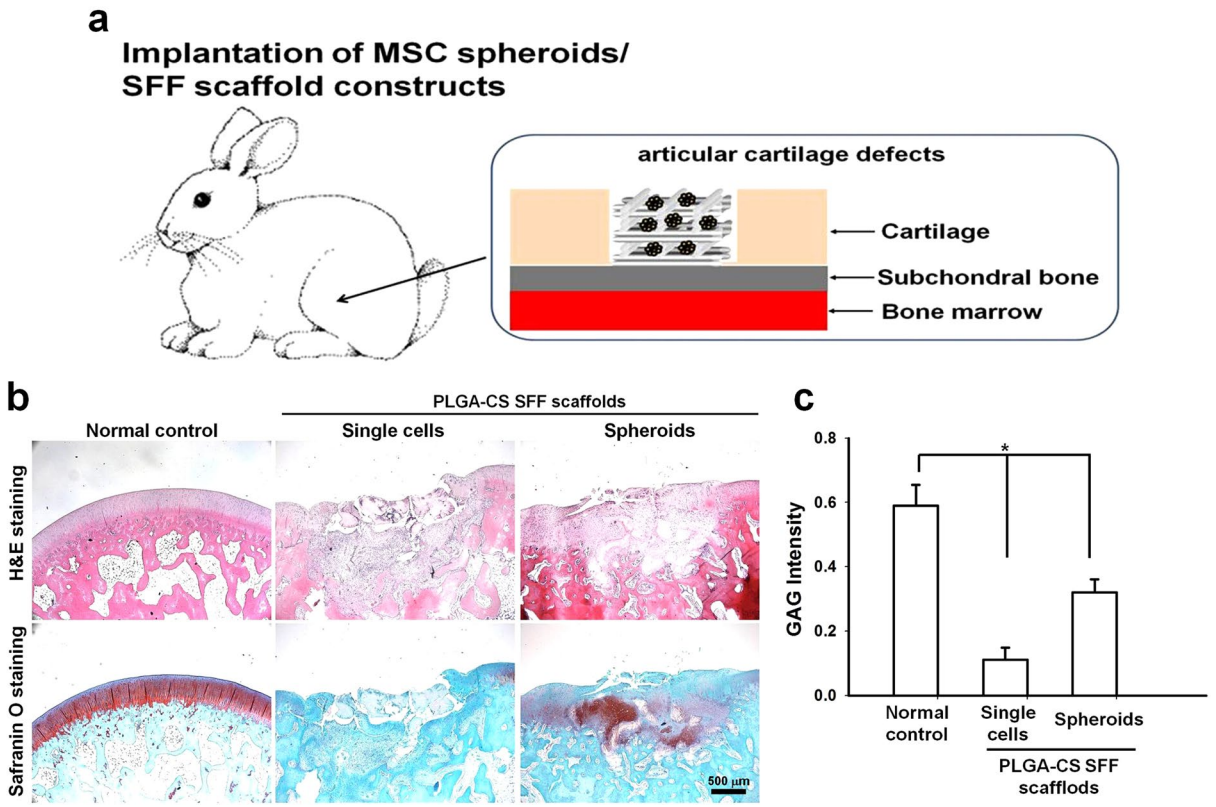

Fig. 9. Rabbit knee articular cartilage regeneration. Spheroids were generated from self-assembly of rabbit adipose-derived adult stem cells on CS-HA membranes. **(a)** Illustration for the implantation of the MSC spheroid/SFF scaffold combined constructs in rabbit knee joints. **(b)** Histological mages based on the typical H&E and Safranin O stained sections from the regenerated cartilage in the chondral defects implanted with single cell-seeded or spheroid-loaded PLGA-CS SFF scaffolds after one month. (c) The intensity of GAG staining quantified from the images. * refers to $p < 0.05$.

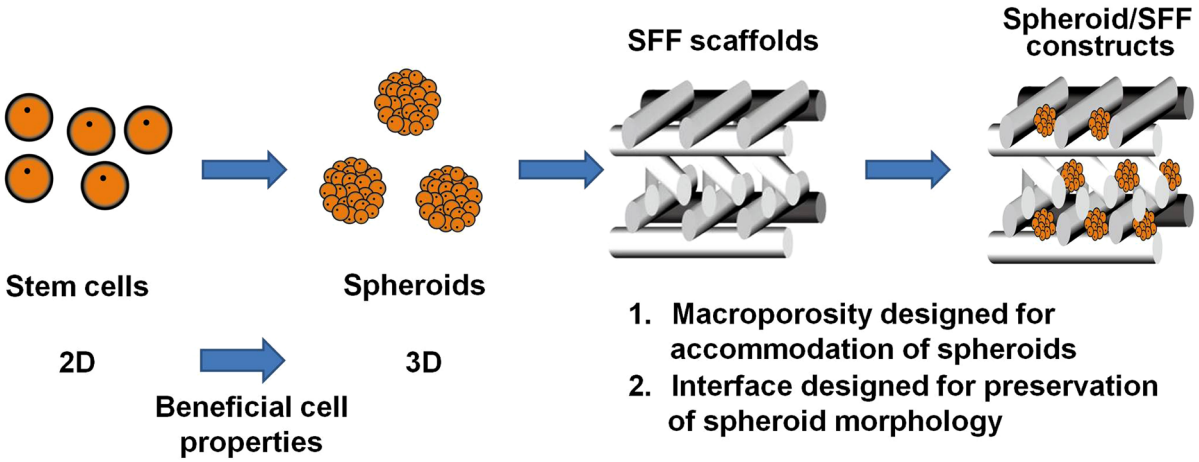

Fig. 10. New perspectives of materials design, i.e., macroporosity and spheroid-sustaining material interface, for fabrication of the next-generation tissue engineered constructs to meet the emerging trend of 3D cell culture.

(Hsu *et al.*, 2012b). The SFF/LFDM scaffolds modified by chitosan effectively preserved the spheroid morphology. For the first time, scaffolds that not only accommodate the MSC spheroids but offer a microenvironment for maintaining the spheroid morphology are conveniently produced. Such design is illustrated in Fig. 10**.**

Substrate-derived MSC spheroids in this study demonstrated an increase in cell-cell interaction *vs.* MSC single cells, through N-cadherin upregulation. It was thus reasonable to assume that a spheroid-sustaining microenvironment should be able to maintain the N-cadherin expression appropriately. Unlike MSC spheroids from suspension culture that only demonstrated a slightly higher level of TGF-β3 mRNA expression *vs.* monolayer (Yoon *et al.*, 2012), our substrate-derived MSC spheroids showed a significant increase in TGF-β3 and BMP-2 expression. Both N-cadherin and TGF-β3 upregulation have been associated with enhanced chondrogenesis (Goldring *et al.*,

2006). The necessity to preserve the spheroid morphology for enduring the beneficial effect of 3D spheroids, however, has not been reported so far. Such necessity was first verified by examining the interaction between PLGA, a common tissue engineering polymer, and MSC spheroids in this study. When spheroids became spread cells after replating on PLGA, the beneficial effect on chondrogenic differentiation was quickly lost. Likewise, the maintenance of spheroid morphology within a scaffold was critical to the chondrogenic gene expression and GAG production in the scaffold. Since cadherins and cytokines are important regulators for stem cell biology, we expect that sustaining the 3D morphology would be crucial for the therapeutic effect of cellular spheroids in general.

Two types of MSC spheroids were tested in this study, i.e., CS derived and CS-HA derived spheroids. Both were found to promote the chondrogenic differentiation of MSCs *in vitro* and *in vivo*. CS-HA derived spheroids showed better chondrogenesis than CS derived spheroids. It has been shown that the properties of substrate-derived MSC spheroids were substrate-dependent (Yeh *et al.*, 2012). CS-HA derived MSC spheroids had greater N-cadherin expression and better spheroid morphology than CS derived MSC spheroids, which may account for the better chondrogenic effect presented by CS-HA derived MSC spheroids. Moreover, MSC single cells, CS derived MSC spheroids, and CS-HA derived MSC spheroids each produced ~28, ~82 and ~134 μg of GAGs per PLGA-CS scaffold. The regeneration capacity of MSC spheroids is superior to primary porcine chondrocytes in PLGA SFF scaffolds (producing ~90 μg of GAGs per same-size scaffold after 4 weeks *in vitro* (Yen *et al.*, 2009)).

Although MSC spheroids generated by the other methods such as hanging drops, suspension, or non-adherent surface were also reported to possess beneficial properties over single cells, the translation of *in vitro* results to the *in vivo* environment may be quite challenging because these spheroids tend to spread immediately when no longer residing within the original microenvironment or when in contact with another material surface (Bartosh *et al.*, 2010). This may explain why investigations on 3D MSC spheroids were mainly focused on the *in vitro* properties, not on the successful implementation to animal models. In spite of the rather limited works *in vivo*, MSC spheroids generated by suspension culture were reported to promote vascularisation in mice when directly injected in ischemic hind limb (Bhang *et al.*, 2012). Transplantation of MSC spheroids with Matrigel was found to be more effective in regenerating the nude mice injured sciatic nerves than single cells (Lee *et al.*, 2012). In the current study, we observed that the self-assembled MSC spheroids kept their morphology in scaffolds only when the scaffolds were surface-modified by chitosan. We believed that delivering the microenvironment that sustained the spheroids, along with the spheroids, could be better translated. Indeed, our *in vivo* results showed that MSC spheroids in PLGA-CS SFF scaffolds formed more neocartilage in NOD/SCID mice than single cells in the same scaffolds. Parallel to our *in vitro* results, CS-HA derived spheroids were more effective than CS derived spheroids in producing the cartilage-associated ECM *in vivo* (GAGs >250 μg per scaffold), which corroborates the translatability of our design. In addition, we found that MSC spheroids seemed to recruit more host cells for neotissue formation than MSC single cells did. The *in vitro* chemotactic assay also demonstrated that MSC spheroids recruited more cells, but the extra recruiting ability was abolished in the presence the SDF-1 inhibitor. Therefore, SDF-1 may be a key factor for the host cell recruitment by MSC spheroids observed in NOD/SCID mice.

The better regeneration capacity of MSC spheroids *vs.* single cells in SFF scaffolds was further confirmed in rabbit knee joint implantation. It has been recently shown that transplantation of MSC aggregates generated by hanging drops may help regenerate cartilage in rabbit knee but only at low density. At higher densities, these spheroids failed to regenerate cartilage because of cell death and nutrient deprivation (Suzuki *et al.*, 2012). Scaffolds play a critical role in hyaline cartilage regeneration by improving the survival of transplanted cells (Moutos *et al.*, 2007; Tran *et al.*, 2010). SFF scaffolds are considered better than the conventional scaffolds because of their good mass transport properties (Hollister, 2005; Kim *et al.*, 2012). SDF-1 impregnated in an alginate gel (Sukegawa *et al.*, 2012) or a collagen (Zhang *et al.*, 2013) scaffold was reported to enhance hyaline cartilage regeneration. We therefore suggest that the advantages on mass transport (cell survival) and SDF-1 release (cell recruitment) of the better preserved 3D cellular spheroids may be responsible for the outstanding cartilage regeneration *in vivo* by the novel scaffold/spheroid combination in this study.

SFF belongs to computer-aided 3D printing technology that can produce customised scaffolds. MSCs may be obtained from the adipose tissue of the patients and form spheroids easily. The combination of MSC spheroids and scaffolds may recruit host cells to participate in tissue regeneration. Such a design may reduce the amount of MSCs required for tissue regeneration and minimise *in vitro* manipulation of cells, which increase the possibility to be translated into clinics. On the other hand, the HA solution employed for cell seeding in this study was not cross-linked and may be lost during long term culture or animal studies. This was designed in order not to interfere with the results. It is likely that the MSC spheroids may be better preserved and more functional in HA-based hydrogel (slightly cross-linked) or other materials, which may be a future direction of improvement. Finally, despite the promising results from 1-month animal studies (rabbit joint), data were limited because the quantification was performed through image analysis on histological staining. Long-term results and biochemical analyses are necessary to validate the success of this approach.

Conclusions

We have successfully created a robust delivery carrier with a designed microenvironment for keeping MSC spheroids functional in long term for cartilage tissue engineering. The maintenance of spheroid morphology by proper interfacial materials (such as chitosan) is highly associated with the functions of cellular spheroids *in vitro* and *in vivo*. The

well-kept spheroids express more adhesion molecules, cytokines, and have greater differentiation capacities *in vitro*. The approach is translatable in NOD/SCID mice and in a rabbit chondral defect model. Additionally, the MSC spheroids may recruit host cells to participate in tissue regeneration *in vivo*. This work reveals two new perspectives of design, i.e., macroporosity and spheroid-sustaining material interface, for reproducing the microenvironment in a next-generation tissue-engineering scaffold to meet the emerging trend of 3D multicellular culture.

Acknowledgments

This research was supported by the Program for Stem Cell and Regenerative Medicine Frontier Research (NSC101-2321-B-002-039) sponsored by the National Science Council, Taiwan.

References

Bartosh TJ, Ylostalo JH, Mohammadipoor A, Bazhanov N, Coble K, Claypool K, Lee RH, Choi H, Prockop DJ (2010) Aggregation of human mesenchymal stromal cells (MSCs) into 3D spheroids enhances their antiinflammatory properties. Proc Natl Acad Sci USA **107**: 13724-13729.

Bhang SH, Cho SW, La WG, Lee TJ, Yang HS, Sun AY, Baek SH, Rhie JW, Kim BS (2011) Angiogenesis in ischemic tissue produced by spheroid grafting of human adipose-derived stromal cells. Biomaterials **32**: 2734-2747.

Bhang SH, Lee S, Shin JY, Lee TJ, Kim BS (2012) Transplantation of cord blood mesenchymal stem cells as spheroids enhances vascularization. Tissue Eng Part A **18**: 2138-2147.

Busscher HJ, van der Mei HC, Subbiahdoss G, Jutte PC, van den Dungen JJ, Zaat SA, Schultz MJ, Grainger DW (2012) Biomaterial-associated infection: locating the finish line in the race for the surface. Sci Transl Med **4**: 153rv110.

Chen M, Le DQ, Baatrup A, Nygaard JV, Hein S, Bjerre L, Kassem M, Zou X, Bunger C (2011) Self-assembled composite matrix in a hierarchical 3-D scaffold for bone tissue engineering. Acta Biomater **7**: 2244-2255.

Goldring MB, Tsuchimochi K, Ijiri K (2006) The control of chondrogenesis. J Cell Biochem **97**: 33-44.

Hollister SJ (2005) Porous scaffold design for tissue engineering. Nat Mater **4**: 518-524.

Ho PJ, Yen ML, Tang BC, Chen CT, Yen BL (2013) H2O2 accumulation mediates differentiation capacity alteration, but not proliferative decline, in senescent human fetal mesenchymal stem cells. Antioxid Redox Signal **18**:1895-1905.

Hsu SH, Huang GS, Lin SY, Feng F, Ho TT, Liao YC (2012a) Enhanced chondrogenic differentiation potential of human gingival fibroblasts by spheroid formation on chitosan membranes. Tissue Eng Part A **18**: 67-79.

Hsu SH, Lin CH, Tseng CS (2012b) Air plasma treated chitosan fibers-stacked scaffolds. Biofabrication **4**: 015002.

Hsu SH, Lin YL, Lin TC, Tseng TC, Lee HT, Liao YC, Chiu IM (2012c) Spheroid Formation from Neural Stem Cells on Chitosan Membranes. J Med Biol Eng **32**: 85-90.

Huang GS, Dai LG, Yen BL, Hsu SH (2011) Spheroid formation of mesenchymal stem cells on chitosan and chitosan-hyaluronan membranes. Biomaterials **32**: 6929-6945.

Kim JY, Yoon JJ, Park EK, Kim DS, Kim SY, Cho DW (2009) Cell adhesion and proliferation evaluation of SFF-based biodegradable scaffolds fabricated using a multi-head deposition system. Biofabrication **1**: 015002.

Kim TG, Shin H, Lim DW (2012) Biomimetic Scaffolds for Tissue Engineering. Adv Funct Mater **22**: 2446-2468.

Kirn TG, Park SH, Chung HJ, Yang DY, Park TG (2010) Hierarchically Assembled Mesenchymal Stem Cell Spheroids Using Biomimicking Nanofilaments and Microstructured Scaffolds for Vascularized Adipose Tissue Engineering. Adv Funct Mater **20**: 2303-2309.

Lee EJ, Xu L, Kim GH, Kang SK, Lee SW, Park SH, Kim S, Choi TH, Kim HS (2012) Regeneration of peripheral nerves by transplanted sphere of human mesenchymal stem cells derived from embryonic stem cells. Biomaterials **33**: 7039-7046.

Lee JI, Sato M, Kim HW, Mochida J (2011) Transplantatation of scaffold-free spheroids composed of synovium-derived cells and chondrocytes for the treatment of cartilage defects of the knee. Eur Cell Mater **22**: 275-290.

Moutos FT, Freed LE, Guilak F (2007) A biomimetic three-dimensional woven composite scaffold for functional tissue engineering of cartilage. Nat Mater **6**: 162-167.

Nosal WH, Thompson DW, Sarkar S, Subramanian A, Woollam JA (2005) Quantitative oscillator analysis of IR-optical spectra on spin-cast chitosan films. Spectrosc-Int J **19**: 267-274.

O'Shea TM, Miao X (2008) Bilayered scaffolds for osteochondral tissue engineering. Tissue Eng Part B Rev **14**: 447-464.

Potapova IA, Gaudette GR, Brink PR, Robinson RB, Rosen MR, Cohen IS, Doronin SV (2007) Mesenchymal stem cells support migration, extracellular matrix invasion, proliferation, and survival of endothelial cells *in vitro*. Stem Cells **25**: 1761-1768.

Saha K, Pollock JF, Schaffer DV, Healy KE (2007) Designing synthetic materials to control stem cell phenotype. Curr Opin Chem Biol **11**: 381-387.

Su G, Zhao Y, Wei J, Han J, Chen L, Xiao Z, Chen B, Dai J (2013) The effect of forced growth of cells into 3D spheres using low attachment surfaces on the acquisition of stemness properties. Biomaterials **34**: 3215-3222.

Sukegawa A, Iwasaki N, Kasahara Y, Onodera T, Igarashi T, Minami A (2012) Repair of rabbit osteochondral defects by an acellular technique with an ultrapurified alginate gel containing stromal cell-derived factor-1. Tissue Eng Part A **18**: 934-945.

Suzuki S, Muneta T, Tsuji K, Ichinose S, Makino H, Umezawa A, Sekiya I (2012) Properties and usefulness of aggregates of synovial mesenchymal stem cells as a source for cartilage regeneration. Arthritis Res Ther **14**: R136.

Teixeira LSM, Leijten JCH, Sobral J, Jin R, van Apeldoorn AA, Feijen J, van Blitterswijk C, Dijkstra PJ,

Karperien M (2012) High throughput generated micro-aggregates of chondrocytes stimulate cartilage formation *in vitro* and *in vivo*. Eur Cells Mater **23**: 387-399.

Tran RT, Thevenot P, Zhang Y, Gyawali D, Tang L, Yang J (2010) Scaffold Sheet Design Strategy for Soft Tissue Engineering. Nat Mater **3**: 1375-1389.

Wang W, Itaka K, Ohba S, Nishiyama N, Chung UI, Yamasaki Y, Kataoka K (2009) 3D spheroid culture system on micropatterned substrates for improved differentiation efficiency of multipotent mesenchymal stem cells. Biomaterials **30**: 2705-2715.

Yeh HY, Liu BH, Hsu SH (2012) The calcium-dependent regulation of spheroid formation and cardiomyogenic differentiation for MSCs on chitosan membranes. Biomaterials **33**: 8943-8954.

Yen BL, Huang HI, Chien CC, Jui HY, Ko BS, Yao M, Shun CT, Yen ML, Lee MC, Chen YC (2005) Isolation of multipotent cells from human term placenta. Stem Cells **23**: 3-9.

Yen HJ, Hsu SH, Tseng CS, Huang JP, Tsai CL (2009) Fabrication of precision scaffolds using liquid-frozen deposition manufacturing for cartilage tissue engineering. Tissue Eng Part A **15**: 965-975.

Ylostalo JH, Bartosh TJ, Coble K, Prockop DJ (2012) Human Mesenchymal Stem/Stromal Cells Cultured as Spheroids are Self-activated to Produce Prostaglandin E2 that Directs Stimulated Macrophages into an Anti-inflammatory Phenotype. Stem Cells **30**: 2283-2296.

Yoon HH, Bhang SH, Shin JY, Shin J, Kim BS (2012) Enhanced cartilage formation *via* three-dimensional cell engineering of human adipose-derived stem cells. Tissue Eng Part A **18**: 1949-1956.

Zhang W, Chen J, Tao J, Jiang Y, Hu C, Huang L, Ji J, Ouyang HW (2013) The use of type 1 collagen scaffold containing stromal cell-derived factor-1 to create a matrix environment conducive to partial-thickness cartilage defects repair. Biomaterials **34**: 713-723.

Zorlutuna P, Annabi N, Camci-Unal G, Nikkhah M, Cha JM, Nichol JW, Manbachi A, Bae H, Chen S, Khademhosseini A (2012) Microfabricated biomaterials for engineering 3D tissues. Adv Mater **24**: 1782-1804.

Discussion with Reviewers

M. Fisher: What do you consider optimal *in vitro* cultivation times prior to *in vivo* joint implantation?
Authors: We only performed *in vitro* culture (without TGF-β3) for 3 days. This period was intended for spheroids to adapt to the scaffolds. Since no TFG-β3 was used, the constructs were implanted *in vivo* at 3 days to keep the maximal viability and stemness of the spheroids.

M. Fisher: Please discuss a potential step from bench to bedside!
Authors: Fabrication of SFF scaffolds can be customised based on the shape and size of the patient's defect. Cells may be obtained from a cell bank (placenta-derived stem cells with low immune response) or isolated from the patient's own adipose tissue. Spheroids may be generated *in vitro*, seeded in the customised SFF scaffold, pre-cultured without induction for a short period (about 3 days), and implanted into the patient's defect for clinical cartilage repair.

G. Salzmann: Although the authors suggest a pure chondral defect is created in the rabbit model, there appears to be significant remodelling of the bone. How do the authors explain these results?
Authors: We were very careful during the surgery to avoid a drilling on the bone. However, due to the full depth and the close vicinity, there may be a possibility that some bone was also defected, which caused the remodelling.

Reviewer III: Control experiments with conventional microporous structures should be performed. Additionally, treatment with chitosan is a second important parameter characteristic. Its effect should also be evaluated in a control experiment. Please comment!
Authors: We have compared the seeding efficiency of PLGA microporous scaffolds and chitosan microporous scaffolds (pore size 100-300 μm). The seeding efficiency for single cells was above or approached 50 % (satisfactory). However, the efficiency for spheroids in either type of scaffolds was below 10 %.